Quadrupolar, structural, and magnetic ordering in DyB_2C_2 studied by symmetry analysis and neutron diffraction

O. Zaharko*
Laboratory for Neutron Scattering, ETH Zurich & Paul Scherrer Institute, CH-5232 Villigen PSI, Switzerland

W. Sikora
AGH University of Science and Technology, Faculty of Physics and Nuclear Techniques, 30-059 Krakow, Poland

F. Bialas
Nowy Sacz School of Business NLU, Nowy Sacz, Poland

U. Staub
Swiss Light Source, Paul Scherrer Institute, CH-5232 Villigen PSI, Switzerland

T. Nakamura
Japan Synchrotron Radiation Research Institute, Mikazuki, Sayo, Hyogo 679-5148, Japan
(Received 5 February 2004; revised manuscript received 17 March 2004; published 30 June 2004)

Antiferroquadrupolar (AFQ) and antiferromagnetic (AFM) order in DyB_2C_2 have been investigated by theoretical symmetry analysis and neutron single crystal diffraction experiment with 0 to 4 T applied magnetic field along [100]. New symmetry arguments indicate that the AFQ ordering below $T_Q=24.7$ K is accompanied by structural distortions involving boron and carbon atoms, but not dysprosium ions. In the AFQ phase a new arrangement of quadrupoles is proposed based on symmetry analysis of the long-range quadrupolar ordering, neutron diffraction study of the field-induced dipolar magnetic structure, and other available observations. This is a 90° arrangement of quadrupoles of neighboring atoms in the *xy* plane, and along *z*. For the zero-field AFM phase, the refinement of neutron single crystal diffraction data of $Dy^{11}B_2C_2$ against models proposed by Yamauchi *et al.* [J. Phys. Soc. Jpn. **68**, 2057 (1999)] (model A) and by van Duijn, Attfield, and Suzuki [Phys. Rev. B **62**, 6410 (2000)] (model B) allows to give preference to modified model A. The magnetic moments of the four Dy sublattices are equal and are confined in the *xy* plane. The tilt of the Dy moments from the *x* axis is 36(4)° at (0 0 0) and −112(4)° at the $(\frac{1}{2}\ \frac{1}{2}\ 0)$ site. The angle between the Dy moments adjacent along *z* is 76(6)° and not 90° as proposed originally.

DOI: 10.1103/PhysRevB.69.224417 PACS number(s): 75.25.+z

I. INTRODUCTION

DyB_2C_2 with the tetragonal LaB_2C_2-type structure [space group $P4/mbm$, Fig. 1(a)][1] exhibits a complex interplay of structural, orbital, and magnetic degrees of freedom.[2–4] In zero-field antiferroquadrupolar (AFQ) order sets in at an unusually high temperature of $T_Q=24.7$ K. The superstructure reflections observed in the zero-field AFQ state by resonant and nonresonant x-ray diffraction[3–5] can be indexed by the wave vector $\mathbf{k}_1=[0,0,\frac{1}{2}]$.[6] The $(0\ 0\ l/2)$ reflections are attributed to a long-range ordering of quadrupoles and $(0\ 1\ l/2)$ to the accompanying periodic displacement of atoms. The resulting structure is described by the $P4_2/mnm$ space group with *c*-doubled unit cell, and the point symmetry of Dy ions lowers from $4/m$ to $2/m$.

The quadrupole moments of Dy^{3+} ions may have the $\Gamma_5(O_{yz},O_{zx},O_{xy})$ or $\Gamma_3(O_2^0,O_2^2)$ site symmetry. The AFQ ordering originates from a peculiar crystal electric field scheme. It is proposed[4] and experimentally confirmed[7] that the ground and first excited Kramers doublets are close in energy. The lifting of degeneracy of this apparent pseudoquartet leads to the ordering of quadrupoles below T_Q. According to Tanaka *et al.*,[3] the main axes of quadrupoles are confined in the *xy* plane [Fig. 1(b)] due to the crystal field, and for the ions Dy1(0 0 0) and $\mathrm{Dy2}(\frac{1}{2}\ \frac{1}{2}\ 0)$ are tilted from the *x* axis by angles ϕ and $90-\phi$, while for the quadrupoles of the ions Dy3(0 0 1) and $\mathrm{Dy4}(\frac{1}{2}\ \frac{1}{2}\ 1)$[8] the tilt angles are $90+\phi$ and $-\phi$. Matsumura *et al.*[9] proposed a more symmetric arrangement: the quadrupoles of the Dy ions at $z=0$ are aligned parallel, strictly along $[-110]$, and those at $z=1$ along [110]. This arrangement explained the vanishing of the $(1\ 0\ 5/2)$ reflection in an x-ray resonant diffraction experiment in the AFQ phase.

The structural part of the transition is also a subject of debate. Tanaka *et al.*,[3,10] and Lovesey and Knight,[11] assume that the B and C atoms are displaced along the *z* axis, whereas Hirota *et al.*[4] and Matsumura *et al.*[9] propose that movements of the Dy ions are involved in the transition. We shall try to resolve these issues by symmetry analysis.

Antiferromagnetic (AFM) order develops below $T_N=15.3$ K at zero applied magnetic field. To index the magnetic diffraction pattern in the AFM state two wave vectors, $\mathbf{k}_1=[0,0,\frac{1}{2}]$ and $\mathbf{k}_2=[0,0,0]$, are required.[2] A model (labeled A) of the magnetic structure of $Dy^{11}B_2C_2$ at zero-field was first presented by Yamauchi *et al.*[2] [Fig. 2(a)] based on neutron powder diffraction. Shortly thereafter, van Duijn,

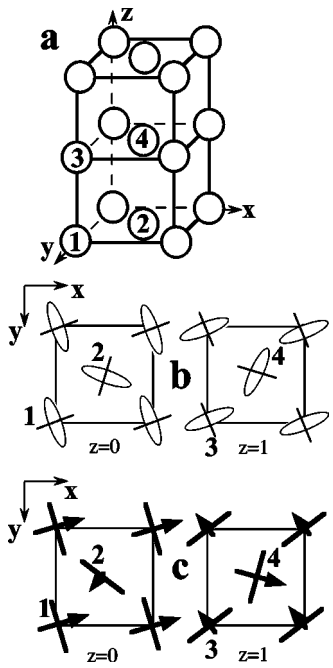

FIG. 1. (a) The crystal structure DyB_2C_2. Only Dy ions are shown and the same labeling is used throughout the paper. (b) The quadrupolar ordering proposed by Tanaka *et al.*[3] (c) Magnetic structure induced in the AFQ state applying $\mathbf{H}\|[100]$, according to Yamauchi *et al.*[15]

Attfield, and Suzuki[12] proposed another model [labeled B, Fig. 2(b)], which fits the data equally well. Both models contain four canted Dy sublattices with magnetic moments confined in the *xy* plane. Canting of the moments results in a ferromagnetic component along [110]. For both models the magnetic moments of the four Dy sublattices have the same magnitude, but they have different symmetry relations between the moments. In model A the magnetic moments of Dy1-Dy4 (Dy2-Dy3) are symmetry related; in model B, the moments of Dy1-Dy3 and Dy2-Dy4 are coupled. The relative orientation of magnetic moments at $z=0$ and $z=1$ is also slightly different for A and B. We performed symmetry analysis and neutron single crystal diffraction of $Dy^{11}B_2C_2$ below T_N at zero-field, attempting to distinguish the correct model.

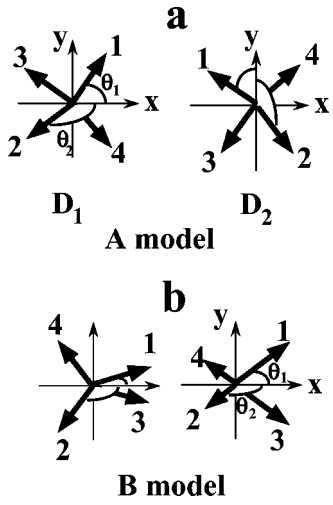

FIG. 2. Diagram of the Dy magnetic moment arrangement (a) A model (left-hand side: domain D_1, right-hand side: domain D_2), (b) B model (left-hand side: proposed by van Duijn, Attfield, and Suzuki, [12] right-hand side: resulting from our study).

The magnetic exchange interactions stabilize either parallel or antiparallel alignments of spins at next-nearest neighbors. While the canted magnetic structure of DyB_2C_2 indicates that the quadrupolar pair interactions favor 90° couplings. The dipolar and quadrupolar interactions are comparable in strength and compete with each other. Application of magnetic field **H** should affect the AFM couplings stronger than the AFQ ones,[13] and indeed, as seen from the magnetic field-temperature phase diagram,[2] applied magnetic field weakly affects the AFQ state, but significantly suppresses the AFM state. In addition, dipolar magnetic moments are induced in the AFQ phase, reflecting the underlying quadrupolar order. This allows the study the AFQ state of $Dy^{11}B_2C_2$ by neutron diffraction.[14,15]

The models of magnetic structures induced by $\mathbf{H}\|$ [100] and [110] have been proposed by Yamauchi *et al.*[2,14] The authors assumed that the dipole moments are perpendicular to the main axis of quadrupole moments, as shown in Fig. 1(c) for $\mathbf{H}\|$ [100]. The induced magnetic structure differs from the zero-field structure by an increase of the *x* components of the Dy1 and Dy4 moments, which align parallel to the field, and decrease of the *x* components of Dy2 and Dy3, which point opposite to the field. However, a comprehensive understanding of the AFQ arrangement and the induced dipolar AFM structure has not been achieved. We extended the available studies and performed a neutron diffraction of $Dy^{11}B_2C_2$ single crystal at moderate magnetic fields (0–4 T) applied along [100]. Our experimental findings allow us to elucidate new details about the induced magnetic structure and the related AFQ ordering.

II. EXPERIMENTAL DETAILS

A single crystal of $Dy^{11}B_2C_2$ enriched with 99.5 at % ^{11}B isotope has been grown by the Czochralski method in an arc furnace with four electrodes. The crystal has been cleaved and a piece with the dimensions $15\times5\times1.2$ mm^3 has been used for further experiments. Enrichment in ^{11}B isotope strongly reduced neutron absorption. However, absorption remained significant due to natural Dy. Neutron intensity has been collected on the single crystal diffractometer TriCS at the spallation neutron source SINQ with a neutron wavelength of $\lambda=1.18$ Å using a ^{3}He area detector. Two experimental setups have been employed. For the zero-field data a four-circle cradle has been used, allowing inspection of a large number of reciprocal points. The crystal has been mounted in a closed cycle ^{4}He refrigerator. For measurements under magnetic field a vertical cryomagnet has been installed. In this setup, reflections scattered ±15° out of the horizontal plane have been measured by tilting the area detector. The crystal has been mounted with the [100] direction vertically and the magnetic field has been applied in the same direction. The crystal was well fixed to avoid any

movement due to the ferromagnetic component expected under an applied field. Measurements have been performed in a field cooled state. This means for every measurement with a new field value the crystal was heated to 30 K, a field was applied, and the crystal was cooled to 5 K. The temperature dependence of Bragg peaks was measured upon heating the crystal.

The single crystal of good quality has been chosen for the experiment. But successive heating and cooling led to the splitting of the crystal perpendicular to c witnessed by the split of the Bragg peaks of the type $(0\,0\,l)$ and (hkl), with l large. We decided to proceed with the crystal but to increase scanning ranges to get a reliable background, and then integrated all intensity above the background.

III. RESULTS AND DISCUSSION

A. Symmetry analysis of the AFQ phase below T_Q

To resolve existing ambiguities about the quadrupolar and structural transitions at T_Q, we performed a group theoretical analysis.[17–21] The symmetry analysis allows us to describe changes of different physical properties during the transition based on the symmetry of the parent phase ($P4/mbm$) and the wave vector involved in the transition ($\mathbf{k}_1=[0,0,\frac{1}{2}]$). It supplies the coordinate system, which reflects the symmetry of the problem in the best way and provides the simplest form of description of possible structures. This coordinate system is formed by the basis vectors $\Psi_{\mathbf{k}_L,\nu,\lambda}$ of irreducible representation (IR) of the symmetry group G of the parent structure. Any property $\mathbf{S}$ of the crystal can be described in such a coordinate system as a linear combination of the basis vectors of IR of the group G:

$$\mathbf{S}^{\mathbf{k}_L}=\sum_{\mathbf{k}_L}\sum_{\nu=1,j}\sum_{\lambda=1,i}C_{\mathbf{k}_L,\nu,\lambda}\Psi_{\mathbf{k}_L,\nu,\lambda}, \tag{1}$$

where $\mathbf{k}_L$ is the wave vector, ν the number of representations, and λ runs over the dimensions of IR. The sets of the coefficients C, being the components of the studied property, restrict the number of free parameters and, as a result, reduce the number of possible structures. The correct linear combination of coefficients is the order parameter of the corresponding transition. We involved the program MODY[22] to calculate possible solutions.

First, we consider the structural transition. For Dy ions, occupying the $2(a)$ site, three irreducible representations are possible; τ_2, τ_4, τ_{10}. The allowed displacements and corresponding symmetry after the transition are presented in Table I. Two IR, τ_2 and τ_4, would be consistent with the z shifts of the Dy ions proposed by Matsumura *et al.*[9] However, special reflection conditions $hkl:h+k=2n$ of the two corresponding space groups, $P42_12$ and $P4bm$, are not compatible with the observation of the $(0\,1\,l/2)$ reflections by x-ray diffraction.[3,4] The τ_{10} representation would lead to the displacements along x and an orthorhombic or monoclinic space group. It is unlikely, therefore, that the Dy ions are involved in the structural part of the transition.[23]

For the $4(h)$ positions occupied by the B and C atoms the symmetry analysis allows eight representations: τ_1, τ_2, τ_4, $\tau_6-\tau_{10}$ (see Table II). The τ_1, τ_7, and τ_{10} representations correspond to the shifts of the B and C atoms along the z axis, others to the shifts in the xy plane. The τ_1, τ_2, τ_4, and τ_8 IR lead to the space groups with the extinction conditions contradicting the observed $(0\,1\,l/2)$ reflections. The τ_6, τ_9, and τ_{10} representations lead to too low symmetry. For example, τ_6 results in the $P42_1m$ space group, which besides the $(0\,1\,l/2)$ reflections would allow $(0\,0\,l/2)$. The $(0\,0\,l/2)$ reflections are, in fact, observed in an x-ray diffraction experiment, but they originate not from periodic lattice distortions, but from the anisotropy of atomic scattering amplitude of Dy (so-called Templeton-Templeton scattering).[11] Therefore, they are related to the quadrupolar ordering and not directly to the structural part of the transition.

TABLE I. Symmetry analysis of the structural transition for DyB_2C_2 (space group $P4/mbm$) associated with $\mathbf{k}_1=[0,0,\frac{1}{2}]$ for the $2(a)$ site occupied by Dy ions with coordinates Dy1: (0 0 0) and Dy2: $(\frac{1}{2}\,\frac{1}{2}\,0)$. c, c_1, and c_2 are real coefficients used as order parameter, IR—irreducible representation, SG—space group after transition.

IR	Dy1	Dy2	SG
τ_2	$(0\,0\,c)$	$(0\,0\text{-}c)$	D_4^2-$P42_12$
τ_4	$(0\,0\,c)$	$(0\,0\,c)$	$C_{4\nu}^2$-$P4bm$
τ_{10}	$(c_1\,0\,0)$	$(c_1\,0\,0)$	C_{2h}^2-$P2_1m$, C_s^1-Pm
	$(c\,0\,0)$	$(c\,0\,0)$	$C_{2\nu}^2$-$Pmc2_1$

Summarizing, only the τ_7 representation describes fully the experimental observations. It leads to a structure with the $P4_2/mnm$ symmetry with the B and C atoms displaced along the z axis and no shifts of the Dy ions.

Let us now analyze possible schemes of the quadrupolar ordering. Up to now in the literature[3–5] only the site symmetry has been considered. Here we involve also the translational symmetry in the analysis. The potential of continuous charge distribution $\rho(r)$ in DyB_2C_2 may be presented as follows:

$$\Phi(r)=\Phi_0(r)+\Phi_Q(r), \tag{2}$$

where $\Phi_0(r)$ is a potential of the spherical symmetry, and $\Phi_{Q(r)}$ is a deformation following from the quadrupolar momentum. The quadrupole moments associated with the $4f$ electron wave functions can be described by the second rank tensor,

$$Q_{ij}=\int(3x_ix_j-r^2\delta_{ij})\rho(r)d^3x. \tag{3}$$

The quadrupolar moment tensor (QMT) has the following properties: the components of QMT are real, the matrix of QMT is symmetric ($Q_{ij}=Q_{ji}$), and the trace of QMT is zero ($\Sigma Q_{ii}=0$). The shape of the surface associated with the deformed potential has twofold-symmetry axes a_1, a_2, and a_3 perpendicular to each other. In general a_1 is different from a_2 and from a_3. These axes form the local coordinate system in which the matrix of QMT is diagonal. The change of the sign of QMT components changes the surface. It becomes flat-

TABLE II. Symmetry analysis of the structural transition for DyB_2C_2 (space group P/mbm) associated with $\mathbf{k_1}=[0,0,\frac{1}{2}]$ for the 4 (h) site occupied by B and C atoms with coordinates 1: $(-x+\frac{1}{2}\ x\ \frac{1}{2})$, 2: $(-x\ -x+\frac{1}{2}\ \frac{1}{2})$, 3: $(x\ x+\frac{1}{2}\ \frac{1}{2})$, and 4: $(x+\frac{1}{2}\ -x\ \frac{1}{2})$, $x_B=0.137$, $x_C=0.339$. c, $\gamma=\cos\phi$, $\sigma=\sin\phi$ are the order parameters, IR—irreducible representation, SG—space group after transition.

IR	1	2	3	4	SG
τ_1	(0 0 c)	(0 0 c)	(0 0 c)	(0 0 c)	D_{4h}^5-$P4/mbm$
τ_2	(c c 0)	(-c c 0)	(c-c 0)	(-c-c 0)	D_4^2-$P42_12$
τ_4	(c-c 0)	(c c 0)	(-c-c 0)	(-cc 0)	C_{4v}^2-$P4bm$
τ_6	(c-c 0)	(-c-c 0)	(c c 0)	(-c c 0)	D_{2d}^3-$P\bar{4}_1m$
τ_7	(0 0 c)	(0 0-c)	(0 0-c)	(0 0 c)	D_{4h}^{14}-$P4_2/mnm$
τ_8	(c c 0)	(c-c 0)	(-c c 0)	(-c-c 0)	D_{2d}^7-$P\bar{4}b2$
τ_9	(γ γ 0)	(-σ σ 0)	(γ γ 0)	(-σ σ 0)	C_{2h}^2-$P2_1/m$, C_i-$P\bar{1}$
τ_{10}	(0 0 γ)	(0 0 σ)	(0 0-σ)	(0 0-γ)	C_{2h}^2-$P2_1/m$, C_s^1-Pm

tened in the direction where it was elongated before, and vice versa.

According to the MODY calculations five irreducible representations are possible for the quadrupolar ordering at the $2(a)$ site: τ_1, τ_3, τ_5, τ_7, and τ_9. The form of the coefficients C of the basis vectors [Eq. (1)] and the QMT matrices are presented in Table III. The corresponding potential distribution deviating from the spherical symmetry is shown in Fig. 3.

Let us consider the τ_7 representation, which fulfills the experimental conditions, in more detail. It is active in the simultaneous structural transition, and the schemes of AFQ ordering emerging from it include also the schemes proposed by Tanaka *et al.*[3] and Matsumura *et al.*[9] The coefficients C acting as an order parameter may adopt the form: $(c_1,0)$, $(0,c_2)$, and (c_1,c_2). If $(c_1,0)$ is the order parameter, the QMT matrices for the ions Dy1 at (0, 0, 0) and Dy2 at $(\frac{1}{2},\frac{1}{2},0)$ are

$$Q=\begin{vmatrix} \pm c_1 & 0 & 0 \\ 0 & \mp c_1 & 0 \\ 0 & 0 & 0 \end{vmatrix}.$$

The charge distribution deformed due to the quadrupolar momentum is elongated along y and x for Dy1 and Dy2, respectively. Because of the wave vector $\mathbf{k}_1=[0,0,\frac{1}{2}]$,[6] the QMT components of the Dy3 and Dy4 ions translated by the lattice vector (001) have the same value but the opposite sign to the QMT components of the Dy1, and Dy2 ions. Therefore, the shape of the charge distribution changes. The charge distribution elongated for Dy1 flattens for Dy3 along y. The QMT matrix translated by the lattice vectors (100) and (010) do not change the shape. The resulting ordering pattern is shown in Fig. 4(a). The main axis of elongation of the Dy charge distribution is 90° rotated for the nearest neighbors, therefore we name this scheme "a 90° arrangement." The structural distortion and the quadrupolar ordering develop simultaneously. Therefore, the displacement of the B and C atoms and the ordering of quadrupoles should correlate. The 90° quadrupolar arrangement implies opposite displacement of the B and C atoms denoted (1) in Table II, as is visible in Fig. 4(a). Such shifts have been proposed by Tanaka[10,24] and Adachi.[5]

For the order parameter $(0,c_2)$ the charge distribution is elongated along $[-110]$ for both Dy1 and Dy2, and along [110] for Dy3 and Dy4. Such an arrangement has been proposed by Matsumura *et al.*[9] and is presented in Fig. 4(b). It implies parallel axes of elongation of charge distribution within the xy plane and a 90° rotation between the adjacent planes at $z=0$ and $z=1$; we would name it "a parallel arrangement". Such a scheme of quadrupolar ordering is compatible with the displacement of the B1 and C1 atoms in the same direction along z.

For the order parameter (c_1,c_2) the asymmetry of the charge distribution is canted in the xy plane. The main axes of elongation of the Dy1 and Dy2 charge distributions are tilted by the angles φ and $90-\varphi$ from the x axis [see Fig. 4(c)]. The charge distribution for the Dy3 (Dy4) ions is flattened in the direction of elongation of the Dy1 (Dy2) charge distribution and is elongated in the perpendicular direction. This scheme of quadrupolar ordering is proposed by Tanaka,[3] which we would name scheme "a canted arrangement." This arrangement coincides with the magnetic structure below T_N, but is asymmetric relative to displacements of the B and C atoms as in the opposite, so in the same direction along z.

We conclude on the basis of symmetry analysis that the τ_7 representation is active in the structural transition involving the B and C atoms, but not the Dy ions, and in the ordering of Dy quadrupoles. The resulting structure has $P4_2/mnm$ symmetry. Three schemes of quadrupolar ordering emerge from symmetry analysis. We propose the relations between these schemes of quadrupolar ordering and displacements of the B and C atoms. It would be of interest, therefore, to study the displacements of atoms below T_Q experimentally, as it would help to distinguish the scheme of quadrupolar ordering in the AFQ phase.

B. Magnetic structure below T_N at $H=0$ T

We consider now the magnetic ordering of DyB_2C_2 at zero-field by means of symmetry analysis. Later we analyze

TABLE III. Symmetry analysis of the quadrupolar transition for DyB_2C_2 (space group $P4/mbm$) associated with $\mathbf{k_1}=[0,0,\frac{1}{2}]$ for the 2(a) site occupied by Dy1 and Dy2 ions. Notations used: IR—irreducible representation, OP—order parameter, SG—space group after transition, $e_1=e^{i\phi_1}$, $e_2=e^{i\phi_2}$, $\gamma_1=\cos\phi_1$, $\gamma_2=\cos\phi_2$, $\sigma_1=\sin\phi_1$, $\sigma_2=\sin\phi_2$, $\overline{\gamma_k}=-\gamma_k$, c, c_1, c_2, a, b—order parameters.

IR	OP	Dy1	Dy2	SG
τ_1	(c 0-c)	$\begin{vmatrix} \frac{1}{2} & 0 & 0 \\ 0 & \frac{1}{2} & 0 \\ 0 & 0 & -1 \end{vmatrix}$	$\begin{vmatrix} \frac{1}{2} & 0 & 0 \\ 0 & \frac{1}{2} & 0 \\ 0 & 0 & -1 \end{vmatrix}$	D_{4h}^5-$P4/mbm$
τ_3	(c 0-c)	$\begin{vmatrix} \frac{1}{2} & 0 & 0 \\ 0 & \frac{1}{2} & 0 \\ 0 & 0 & -1 \end{vmatrix}$	$\begin{vmatrix} -\frac{1}{2} & 0 & 0 \\ 0 & -\frac{1}{2} & 0 \\ 0 & 0 & 1 \end{vmatrix}$	D_{4h}^6-$P4/mnc$, C_{4h}^1-$P4/m$, C_{4h}^5-$I4/m$
τ_5	(c_1 0)	$\begin{vmatrix} c_1 & 0 & 0 \\ 0 & -c_1 & 0 \\ 0 & 0 & 0 \end{vmatrix}$	$\begin{vmatrix} c_1 & 0 & 0 \\ 0 & -c_1 & 0 \\ 0 & 0 & 0 \end{vmatrix}$	D_{4h}^{13}-$P4_2/mbc$
	(0 c_2)	$\begin{vmatrix} 0 & c_2 & 0 \\ c_2 & 0 & 0 \\ 0 & 0 & 0 \end{vmatrix}$	$\begin{vmatrix} 0 & -c_2 & 0 \\ -c_2 & 0 & 0 \\ 0 & 0 & 0 \end{vmatrix}$	D_{4h}^{13}-$P4_2/mbc$
	(c_1 c_2)	$\begin{vmatrix} c_1 & c_2 & 0 \\ c_2 & -c_1 & 0 \\ 0 & 0 & 0 \end{vmatrix}$	$\begin{vmatrix} c_1 & -c_2 & 0 \\ -c_2 & -c_1 & 0 \\ 0 & 0 & 0 \end{vmatrix}$	D_{4h}^{13}-$P4_2/mbc$
τ_7	(c_1 0)	$\begin{vmatrix} c_1 & 0 & 0 \\ 0 & -c_1 & 0 \\ 0 & 0 & 0 \end{vmatrix}$	$\begin{vmatrix} -c_1 & 0 & 0 \\ 0 & c_1 & 0 \\ 0 & 0 & 0 \end{vmatrix}$	D_{4h}^{14}-$P4_2/mnm$
	(0 c_2)	$\begin{vmatrix} 0 & c_2 & 0 \\ c_2 & 0 & 0 \\ 0 & 0 & 0 \end{vmatrix}$	$\begin{vmatrix} 0 & c_2 & 0 \\ c_2 & 0 & 0 \\ 0 & 0 & 0 \end{vmatrix}$	D_{4h}^{14}-$P4_2/mnm$
	(c_1 c_2)	$\begin{vmatrix} c_1 & c_2 & 0 \\ c_2 & -c_1 & 0 \\ 0 & 0 & 0 \end{vmatrix}$	$\begin{vmatrix} -c_1 & c_2 & 0 \\ c_2 & c_1 & 0 \\ 0 & 0 & 0 \end{vmatrix}$	D_{4h}^{14}-$P4_2/mnm$
τ_9	$\begin{pmatrix} c_1e_1 & c_2e_2 \\ c_2e_2 & c_1e_1 \end{pmatrix}$	$a\begin{vmatrix} 0 & 0 & \gamma_1 \\ 0 & 0 & \sigma_1 \\ \gamma_1 & \sigma_1 & 0 \end{vmatrix}$	$b\begin{vmatrix} 0 & 0 & \overline{\gamma_2} \\ 0 & 0 & \sigma_2 \\ \overline{\gamma_2} & \sigma_2 & 0 \end{vmatrix}$	C_{2h}^2-$P2_1/m$

the experimental neutron diffraction data on a $Dy^{11}B_2C_2$ single crystal, taking special care about the absorption correction. For the symmetry analysis of magnetic ordering the AFQ phase of DyB_2C_2 should be taken as the starting phase.[25] The space group of the AFQ phase $P4_2/mnm$ requires doubling of the c period already in the paramagnetic state, and all magnetic peaks are described then by the wave vector $\mathbf{k}_2=[0,0,0]$. The ions Dy1…Dy4 in $P4_2/mnm$ have coordinates $(\frac{1}{2}\ 0\ 0)$, $(0\ \frac{1}{2}\ 0)$, $(\frac{1}{2}\ 0\ \frac{1}{2})$, and $(0\ \frac{1}{2}\ \frac{1}{2})$ and belong to the same crystallographic site 4(c). The wave vector $\mathbf{k}_2$ does not split this position; all four ions belong to the same orbit. Five irreducible representations are obtained for $P4_2/mnm$ and $\mathbf{k}_2=[0,0,0]$. Four real one-dimensional representations, τ_1, τ_3, τ_5, and τ_7, would lead to the easy moment direction along z. This is inconsistent with experimental results. The complex two-dimensional representation τ_9

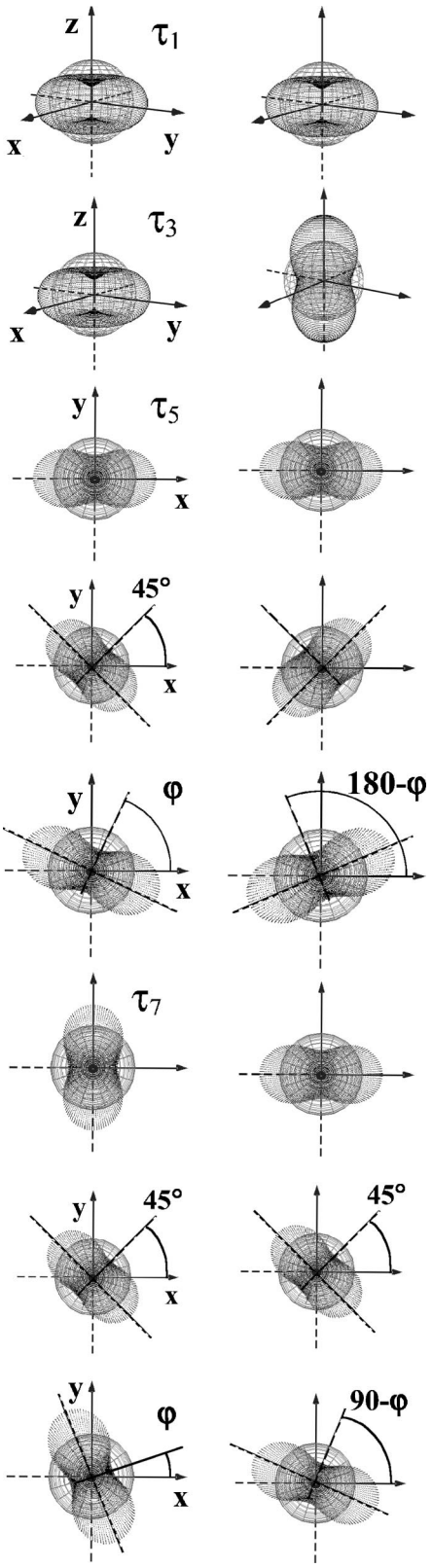

FIG. 3. Spheroids associated with the quadrupolar moment tensor for the τ_1, τ_3, τ_5, and τ_7 representations. The raws in the figure correspond to the raws in Table III; the left column presents spheroids of the Dy1 ion, the right column, those of the Dy2 ion.

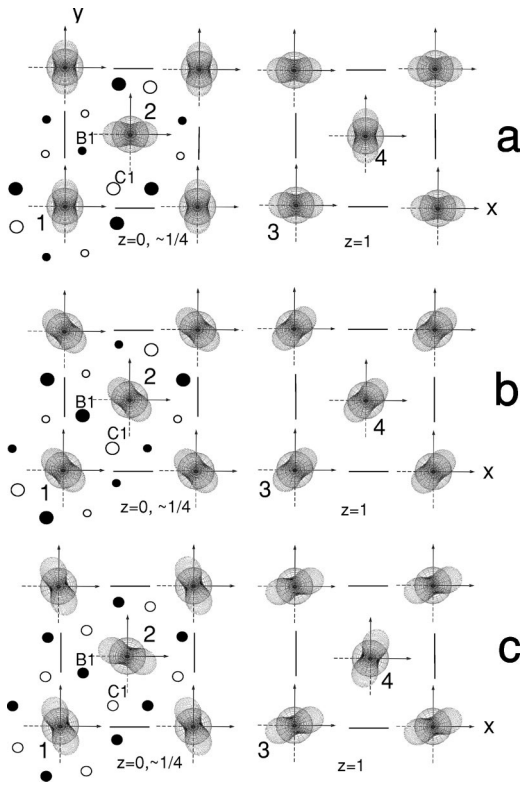

FIG. 4. The long-range ordering of charge distribution of Dy ions deviating from the spherical symmetry due to the quadrupolar momentum for the τ_7 representation for the order parameters: (a) $(c_1,0)$, (b) $(0,c_2)$, and (c) (c_1, c_2). The average spherical charge distribution is also shown. In addition to the Dy charge distributions at $z=0$, the upward (large circles) and downward (small circles) displacements of boron (solid) and carbon (empty) atoms from $z=\frac{1}{2}$ are presented in the left side. (a) The shifts are upward for B1 and downward for C1, (b) both shifts are upwards, and (c) there is no correlation between the Dy charge distribution and displacement of the B and C atoms.

allows magnetic moments within the *xy* plane. The magnetic structure for the τ_9 representation is given by the vectors $\mathbf{S}_1 \ldots \mathbf{S}_4$ for the Dy1…Dy4 ions,

$$\mathbf{S}_1 = c_1 \cos\ \phi_1 \mathbf{e}_x + c_3 \cos\ \phi_3 \mathbf{e}_y,$$

$$\mathbf{S}_2 = -\, c_4 \sin\ \phi_4 \mathbf{e}_x - c_2 \sin \phi_2 \mathbf{e}_y,$$

$$\mathbf{S}_3 = -\, c_3 \sin \phi_3 \mathbf{e}_x + c_1 \sin\ \phi_1 \mathbf{e}_y,$$

$$\mathbf{S}_4 = c_2 \cos\ \phi_2 \mathbf{e}_x - c_4 \cos\ \phi_4 \mathbf{e}_y. \qquad (4)$$

This magnetic structure has eight free parameters and is the most general, as it is derived solely from the symmetry considerations. The real magnetic structure may be more symmetric due to a hidden symmetry of exchange interactions and close energy of pseudoquartet levels. We try, therefore, to impose constraints similar to the ones adopted in models A and B.

Under the assumption that $c_1=c_2$, $c_3=c_4$ and $\phi_1=\phi_2$, $\phi_3=\phi_4$, we obtain a model similar to model A:

$$\mathbf{S}_1 = c_1\cos\,\phi_1\mathbf{e}_x + c_3\cos\,\phi_3\mathbf{e}_y,$$

$$\mathbf{S}_2 = -c_3\sin\,\phi_3\mathbf{e}_x - c_1\sin\,\phi_1\mathbf{e}_y,$$

$$\mathbf{S}_3 = -c_3\sin\,\phi_3\mathbf{e}_x + c_1\sin\,\phi_1\mathbf{e}_y,$$

$$\mathbf{S}_4 = c_1\cos\,\phi_1\mathbf{e}_x - c_3\cos\,\phi_3\mathbf{e}_y. \quad (5)$$

The exact model A, as introduced by Yamauchi *et al.*[2] is obtained when all magnetic moment values are equal, so when $\phi_1=\phi_3=45°$,

$$\mathbf{S}_1 = M_1\mathbf{e}_x + M_3\mathbf{e}_y,$$

$$\mathbf{S}_2 = -M_3\mathbf{e}_x - M_1\mathbf{e}_y,$$

$$\mathbf{S}_3 = -M_3\mathbf{e}_x + M_1\mathbf{e}_y,$$

$$\mathbf{S}_4 = M_1\mathbf{e}_x - M_3\mathbf{e}_y. \quad (6)$$

Note that in this case the magnetic moments of all Dy ions are related and have the same value. The angle between the Dy1 and Dy3 moments is fixed to 90°.

A model similar to model B will follow from assumptions that $c_1=-c_4$, $c_2=c_3$ and $\phi_1=\phi_4-90$, $\phi_3=\phi_2-90$:

$$\mathbf{S}_1 = c_1\cos\,\phi_1\mathbf{e}_x + c_3\cos\,\phi_3\mathbf{e}_y,$$

$$\mathbf{S}_2 = -c_3\sin\,\phi_3\mathbf{e}_x - c_1\sin\,\phi_1\mathbf{e}_y,$$

$$\mathbf{S}_3 = c_1\cos\,\phi_1\mathbf{e}_x - c_3\cos\,\phi_3\mathbf{e}_y,$$

$$\mathbf{S}_4 = -c_3\sin\,\phi_3\mathbf{e}_x + c_1\sin\,\phi_1\mathbf{e}_y, \quad (7)$$

and, additionally, when $\phi_1=\phi_3=45°$,

$$\mathbf{S}_1 = M_1\mathbf{e}_x + M_3\mathbf{e}_y,$$

$$\mathbf{S}_2 = -M_3\mathbf{e}_x - M_1\mathbf{e}_y,$$

$$\mathbf{S}_3 = M_1\mathbf{e}_x - M_3\mathbf{e}_y,$$

$$\mathbf{S}_4 = -M_3\mathbf{e}_x + M_1\mathbf{e}_y. \quad (8)$$

However, the exact B model as proposed by van Duijn, Attfield, and Suzuki[12] cannot be obtained within the τ_9 representation. Similarly to model A, the assumption that all Dy have the same moment value implies symmetry relation between all Dy moments and the angle between the Dy1 and Dy4 moments must be 90°.

Now let us consider the possibility of domain formation for these magnetic structures. As the wave vector $\mathbf{k}_2$ transforms into itself by the symmetry operators of the paramagnetic group $P4_2/mnm$ the configuration domains (*K* domains)[26] are not possible. However, four orientation domains (*S* domains), D_2-D_4, can form due to loss of the fourfold axis. They can be superimposed by a successive 90° rotation. The pairs of domains D_1-D_3 and D_2-D_4 are related by the inversion and cannot be distinguished by the conventional diffraction experiment, so, in the following, we mention only the D_1 and D_2 domains. The arrangement of the magnetic moments in the D_1 and D_2 domains for model A is shown in Fig. 2(a). The D_1 domain produces a net magnetic moment along the *x* axis, while the D_2 domain does so along the *y* axis. The intensity measured from such a multidomain single crystal would be a superposition of intensities generated by these domains.

Finally, we present the refinement of models emerging from theoretical analysis against single crystal neutron diffraction data. Two sets of reflections have been measured at 30 and 12 K. We want to recall that absorption of neutrons in this experiment was severe. This forced us to measure the same reflections several times, at different azimuthal angles Ψ on cost of the number of the independent reflections. The absorption correction for a given shape of the single crystal has been calculated by the Gaussian integration method using the program JANA2000.[27] The correction has been checked with a set of reflections measured varying the angle Ψ. The largest deviation of the as-measured intensity within the Ψ scan was 80%. It reduced to 12% after the absorption correction. This would be considered a poor statistic for a standard data set, but is rather good for the $Dy^{11}B_2C_2$ case. The refinement of crystal and magnetic structures has been performed by the program FULLPROF.[28] The refinement of crystal structure at 30 K converged to $R_F=6.7\%$ for six independent reflections. The only refined parameter, the scale factor, has been used for the magnetic structure refinement.[29] The refinement for two models given by Eqs. (5) and (7) converged to the same R_F value of 15.8%, with equal population of the domains D_1 and D_2 for 16 independent reflections at 12 K.

For the model of Eq. (5) (modified model A) the refined magnetic moment values are 5.67(40) and $5.70(40)\mu_B$ for the Dy1/Dy4 and Dy2/Dy3 pairs, respectively.[30] This confirms the same moment value for all Dy ions. The tilt angles of the Dy1 and Dy2 moments from the *x* axis are $\theta_1=36(4)°$ and $\theta_2=-112(4)°$, respectively. So the canting between the two pairs is 76(6)°, in agreement with Kaneko *et al.*[31] and not 90° as proposed originally by Yamauchi *et al.*[2]

For the model of Eq. (7) (modified model B) the refined magnetic moment values are 3.852 and $7.03(40)\mu_B$ for the Dy1/Dy3 and Dy2/Dy4 pairs, respectively. The tilt angles of the Dy1 and Dy2 moments from the *x* axis are $\theta_1=38(6)°$ and $\theta_2=-142(3)°$. This leads to the canting angle of 104(7)° between the two pairs. The symmetry constraints of model B can be realized only with two distinct magnetic moment values as presented in the right-hand side of Fig. 2(b).

To conclude, our symmetry analysis and neutron single crystal diffraction are consistent with two models: modified model A and modified model B. The first model implies the same magnetic moment value for all Dy ions, but canting between the Dy1/Dy4 and Dy2/Dy3 pairs. The second model suggests two distinct moment values, as well as the presence of canting. We give preference to modified model A. We do not see presently a reason why Dy ions should have different magnetic moment values. They occupy the

same crystallographic site 4(*c*), have the same deformation of local surrounding due to shifts of the B and C atoms, and have the same asymmetry of the change distribution due to the quadrupolar momentum. It is worth noting that the Mössbauer spectra measured below T_N (Ref. 32) were interpreted well by a single set of hyperfine parameters, implying the same moment value for all Dy ions, which supports our proposal.

C. Evolution of AFM peaks as a function of field and temperature in the AFQ and AFM states

We focus now on magnetic ordering in the AFQ state induced by a magnetic field applied along the [1 0 0] direction. The intensity of (0 1 0), (0 0 1), (0 0 1/2), and (0 1 −1/2) reflections in the 5–30 K temperature range, at selected values of magnetic field, is presented in Fig. 5. At zero field, intensity of all peaks decreases with increase of temperature and vanishes around $T_N \sim 16$ K. Therefore, these peaks are associated with the AFM ordering in agreement with previously published neutron diffraction results.[2,12,14,15]

When the magnetic field is applied, some reflections, namely (0 0 1) and (0 1 −1/2), extend their presence up to $T \sim 30$ K. This confirms that an AFM order is induced in the AFQ regime. However, the (0 1 0) and (0 0 1/2) reflections do not appear in the AFQ regime, implying that the induced magnetic arrangement differs from the arrangement stable at zero-field below T_N.

The (0 0 1/2) peak is absent in the AFQ regime in the neutron diffraction experiment, but the (0 0 3/2) peak is present in the resonant x-ray diffraction study.[3,4] This is possible only if these reflections originate from the quadrupole ordering. Such origin of the (0 0 *l*/2) reflections was already proposed by Hirota *et al.* in Ref. 4. But interpretation of the resonant x-ray experiment is not straightforward, as the (0 0 *l*/2) reflections may have magnetic and/or quadrupolar origins.[11] Our results confirm the quadrupolar origin of these reflections. The intensity of (0 0 1/2) decreases with increasing H in the AFM state. This decrease means that the corresponding magnetic contribution is suppressed by field. In the following we suggest a model of the AFM arrangement consistent with this observation. The (0 1 0) reflection disappears at very small fields $H \geqslant 0.2$ T, which is due to a redistribution of the D_1 and D_2 domains as will be shown later. This transition, though not reported before, is confirmed by magnetization measurements presented in Fig. 6.

The (0 0 1) reflection has a structural contribution and, therefore, exists at all temperatures. In Fig. 5 only the magnetic contribution is presented. The thermal evolution of this peak is different in the AFQ and AFM phases. It increases in the AFM phase and decreases in the AFQ phase for increasing temperatures. An increase of the field value, however, increases the (0 0 1) intensity.

The strong (0 1 −1/2) reflection exists in both, AFM and AFQ, phases. Its intensity depends on the applied field in a complex manner. In the AFM regime it grows when a field is applied ($0\ \text{T} < H < 1$ T) and then decreases with increase of the field value. In the AFQ regime intensity grows successively with the field value. Interestingly, this reflection has been studied by zero-field resonant x-ray diffraction and has been attributed to the lattice distortion accompanying the AFQ ordering.[3] Our observation indicates that a significant magnetic contribution is associated with this reflection in the AFQ regime in an applied field.

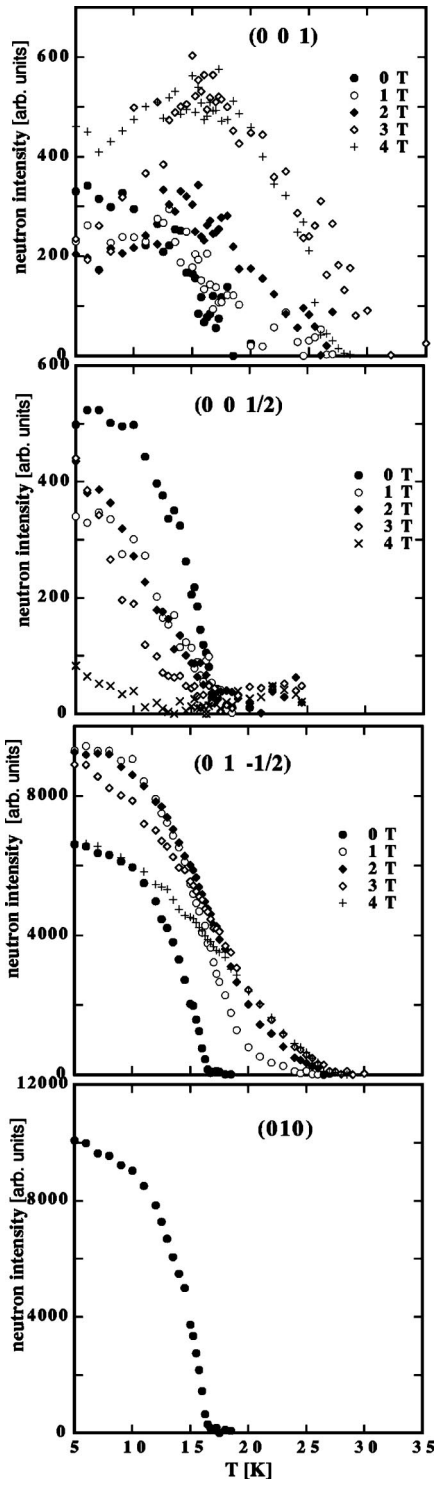

FIG. 5. Temperature dependence of the integrated intensity of (0 0 1), (0 0 1/2), (0 1 −1/2), and (0 1 0) reflections of $Dy^{11}B_2C_2$ with **H**||[100]. The intensities are normalized to the same neutron monitor and the structural contribution to (0 0 1) is subtracted.

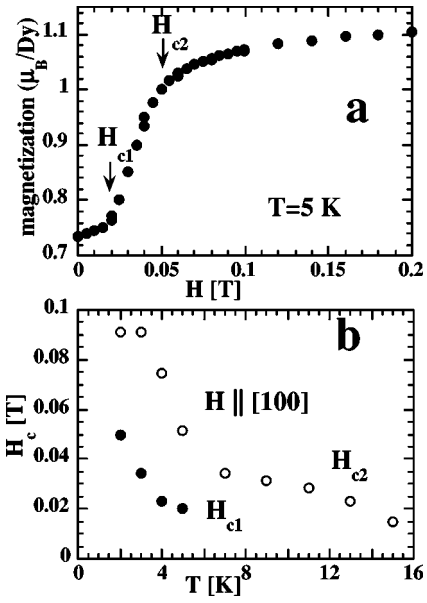

FIG. 6. (a) Magnetization of the $Dy^{11}B_2C_2$ single crystal along [100] at $T=5$ K with two metamagnetic transitions at $H_{c1}=0.02$ T and $H_{c2}=0.05$ T. The origin of one transition is a reorientation of the D_2 domains; the origin of the second transition is not yet established. It may be associated with vanishing of AFQ domains. (b) Temperature evolution of the critical fields H_{c1} and H_{c2}.

To understand the H, T dependence of the magnetic structure it is useful to inspect the contribution of the magnetic moments $\mathbf{M}_1 \ldots \mathbf{M}_4$ of four Dy ions to the magnetic structure factors **F** of the studied reflections. We find that:

$$\mathbf{F_{010}} \sim \mathbf{M}_1 - \mathbf{M}_2 + \mathbf{M}_3 - \mathbf{M}_4,$$

$$\mathbf{F_{001/2}} \sim \mathbf{M}_1 + \mathbf{M}_2 - \mathbf{M}_3 - \mathbf{M}_4,$$

$$\mathbf{F_{001}} \sim \mathbf{M}_1 + \mathbf{M}_2 + \mathbf{M}_3 + \mathbf{M}_4,$$

$$\mathbf{F_{01-1/2}} \sim \mathbf{M}_1 - \mathbf{M}_2 - \mathbf{M}_3 + \mathbf{M}_4. \quad (9)$$

As all four Dy ions contribute to every reflection, it is not possible to derive "model-free" conclusions. However, reasonable constraints may be applied. The negative sign of second-order crystal field Stevens factor[33] indicates a strong planar magnetic anisotropy, which aligns the magnetic moments within the xy plane.[16] The magnetic field in the present experiment has been applied in this plane, $\mathbf{H}\|[100]$. Therefore, we may assume that the ordering and reorientation of the magnetic moments happens only in the xy plane.

Regarding the symmetry relations between the M_x, M_y components it is reasonable to keep the constraints which follow from symmetry analysis and correspond to modified model A. For the D_1 domain presented in Fig. 2(a) (left-hand side) the following relations hold:

$$\mathbf{M_{1x}} = \mathbf{M_{4x}}, \ \mathbf{M_{2x}} = \mathbf{M_{3x}},$$

$$\mathbf{M_{1y}} = -\mathbf{M_{4y}}, \ \mathbf{M_{2y}} = -\mathbf{M_{3y}}, \quad (10)$$

while for the D_2 domain shown in Fig. 2(a) (right-hand side),

TABLE IV. The contribution of the $\mathbf{M_x}$ and $\mathbf{M_y}$ components of the Dy1 and Dy2 ions into the magnetic structure factors **F** for the D_1 and D_2 domains of model A. The evolution of the observed magnetic intensity in the AFQ (I_{AFQ}) and AFM (I_{AFM}) regimes with increase of applied magnetic field H at constant temperature.

	D_1	D_2	I_{AFQ}	I_{AFM}
$\mathbf{F}_{010}$	$\mathbf{M_{1y}}-\mathbf{M_{2y}}$	$\mathbf{M_{1x}}-\mathbf{M_{2x}}$	$I=0$	$I\searrow\searrow$
$\mathbf{F}_{001/2}$	$\mathbf{M_{1y}}+\mathbf{M_{2y}}$	$\mathbf{M_{1x}}+\mathbf{M_{2x}}$	$I=0$	$I\searrow$
$\mathbf{F}_{001}$	$\mathbf{M_{1x}}+\mathbf{M_{2x}}$	$\mathbf{M_{1y}}+\mathbf{M_{2y}}$	$I\nearrow$	$I\nearrow$
$\mathbf{F}_{01-1/2}$	$\mathbf{M_{1x}}-\mathbf{M_{2x}}$	$\mathbf{M_{1y}}-\mathbf{M_{2y}}$	$I\nearrow$	$I\searrow$

$$\mathbf{M_{1x}} = -\mathbf{M_{4x}}, \ \mathbf{M_{2x}} = -\mathbf{M_{3x}},$$

$$\mathbf{M_{1y}} = \mathbf{M_{4y}}, \ \mathbf{M_{2y}} = \mathbf{M_{3y}}. \quad (11)$$

From Eqs. (9) and (10) it follows that for the D_1 domain the magnetic structure factor **F** of the (0, 1, 0) reflection is only sensitive to the y components,

$$\mathbf{F_{010}} \sim \mathbf{M_{1y}} - \mathbf{M_{2y}}, \quad (12)$$

the contributions of the x components cancel. Moreover, the (0 1 0) scattering vector is parallel to the y component of the magnetic moment, and the neutron intensity is zero for this reflection.

For the D_2 domain, only the x components contribute to the (0 1 0) reflection, and the y components cancel:

$$\mathbf{F_{010}} \sim \mathbf{M_{1x}} - \mathbf{M_{2x}}. \quad (13)$$

Therefore, the (0 1 0) reflection has no contribution to the D_1 domain and only the $\mathbf{M_x}$ components contribute from the D_2 domain. Therefore, the observation of the (0 1 0) reflection at zero field below T_N and its vanishing at fields $H \geqslant 0.2$ T suggests that both domains, D_1 and D_2, exist at zero field and that the D_2 domain vanishes when applying a field $\mathbf{H}\|[100]$. Such behavior is favorable, because the net magnetic moment of D_2 is perpendicular to [100]. In the following, for fields $H \geqslant 0.2$ T, we consider only contributions of the D_1 domain. The magnetic structure factors of other studied reflections is presented in Table IV.

We may interpret now the observed variation of the magnetic intensities with field and temperature and try to relate it to the underlying AFQ order. The direction of the induced AFM component and the direction of quadrupoles are defined by the symmetry of the ground state lowered in an applied magnetic field, and the favorable arrangement with the lowest free energy can be obtained by mean-field calculations.[34] The ground state of DyB_2C_2 is not yet known unambiguously, therefore, the relation between the direction of the field-induced moments and quadrupoles is not yet strictly established. We shall assume in the following that the main axis of a deformed charge distribution and the induced magnetic moment of one ion is perpendicular, in accordance with Yamauchi *et al.*[14]

The magnetic structure factor of the (0 0 1/2) reflection is proportional to the sum of the $\mathbf{M_{1y}}$ and $\mathbf{M_{2y}}$ vectors. The absence of the (0 0 1/2) reflection in the AFQ phase means

that the $\mathbf{M_{1y}}$ and $\mathbf{M_{2y}}$ components compensate each other; they are zero or have equal length. Within our assumption on the perpendicular directions of field-induced dipolar moment and quadrupole, the $\mathbf{M_y}$ components should be zero for the 90° arrangement of quadrupoles shown in Fig. 4(a), as $\mathbf{M_{1y}}$ must be zero. For the parallel arrangement of quadrupoles in Fig. 4(b) the $\mathbf{M_y}$ components could be zero or opposite. It is complex, however, to suggest a reason why the $\mathbf{M_{1y}}$ and $\mathbf{M_{2y}}$ components should compensate each other for the canted arrangement of quadrupoles [see Fig. 4(c)].

The intensities of the (0 0 1) and (0 1 −1/2) reflections are related to the difference and the sum of the M_{1x} and M_{2x} values of the D_1 domain, respectively. The increase of the (0 0 1) and (0 1 −1/2) intensities in the AFQ regime with field, means an increase of these differences and sums. So it is reasonable to assume that the moment along the field direction, $\mathbf{M_{1x}}$, increases fast, while the $\mathbf{M_{2x}}$ component does not change significantly. For the 90° arrangement of quadrupoles, such behavior is consistent with the absence of the $\mathbf{M_{2x}}$ component and an increase of $\mathbf{M_{1x}}$. For the canted arrangement, the difference in $\mathbf{M_{1x}}$ and $\mathbf{M_{2x}}$ is also natural.[35] For the parallel arrangement of quadrupoles, however, we see no good reasons why M_{1x} and M_{2x} should be different. We conclude that the AFQ phase observations of the neutron diffraction experiment in an applied magnetic field can be well explained only with the 90° arrangement of quadrupoles.

In the AFM phase at zero field the (0 0 1/2) peak is present; $\mathbf{M_{1y}}$ and $\mathbf{M_{2y}}$ do not compensate each other, implying a canted arrangement of quadrupoles. The canted arrangement is very natural below T_N, as the AFM coupling between neighboring Dy magnetic moments becomes stronger than the 90° coupling between quadrupoles. The decrease of the (0 0 1/2) intensity with increasing **H** in the AFM regime is due to a decrease in the difference of the M_{1y} and M_{2y} values. This implies weakening of the AFM couplings along *y*, with increasing field and possible restoring of the 90° arrangement of quadrupoles stable in the AFQ phase. In the AFM regime the intensity of (0 0 1) increases, and of (0 1 −1/2), decreases. This implies that the net magnetic moment value along *x* (M_{1x}-M_{2x}) increases, with M_{2x} decreasing faster than M_{1x} grows, which is also well understood for the canted arrangement.

Combining information about the $\mathbf{M_x}$ and $\mathbf{M_y}$ components of induced magnetic moments extracted from the neutron diffraction experiment with $\mathbf{H}\|[100]$, we propose the following picture. In the AFQ regime the 90° arrangement of quadrupoles is stable. When magnetic field is applied, the induced $\mathbf{M_{1x}}$ component along the field grows, while the $\mathbf{M_{2x}}$ and $\mathbf{M_y}$ components are absent. In the AFM regime the magnetic exchange interactions couple the neighboring magnetic moments antiferromagnetically. The two conflicting requirements for neighboring Dy ions: (1) 90° coupling of quadrupoles and (2) antiparallel coupling of magnetic moments, lead to frustration of the two orderings and to the canted quadrupolar and magnetic structures. Field applied $\mathbf{H}\|[100]$ tries to align the magnetic moments in its direction and acts, therefore, against AFM couplings. This leads to the difference in the $\mathbf{M_x}$ components: while Dy1 magnetic moment increases, the Dy2 moment decreases. Also, the $\mathbf{M_y}$ component orthogonal to **H** decreases witnessed by a decrease of the (0 0 1/2) intensity with field. We suggest that the quadrupoles rotate back to the arrangement stable in the AFQ phase with an increase of **H**. With temperature lowering, the AFM interactions become stronger and the Dy2 magnetic moment increases. This is why the (0 0 1) intensity, for example, decreases at the constant value of the applied field.

Similar interplay between AFQ and AFM interactions as a function of *T* and *H* may occur for fields applied in the [110] direction. Yamauchi *et al.*[15] reported that the (0 0 1/2) reflection is induced for $1\ \mathrm{T} \leqslant H < 2\ \mathrm{T}$, disappears for $2\ \mathrm{T} \leqslant H < 3\ \mathrm{T}$, and reappears again for $H > 3\ \mathrm{T}$. We suggest that at $2\ \mathrm{T} \leqslant H < 3\ \mathrm{T}$ in the phase IV,[2] the induced magnetic moments point strictly along *x* or *y* directions for the domains D_1 and D_2, respectively. The reappearance of the (0 0 1/2) reflection for $H > 3\ \mathrm{T}$ may indicate rotation of the quadrupoles from the [100]/[010] to [110]/[1-10] directions.

D. Arrangement of quadrupoles at $T_N < T < T_Q$

We now string available arguments trying to resolve, which of the three quadrupolar arrangements is realized in the AFQ phase. The 90° arrangement seems the most probable to us. The reasons are the following: (i) it implies the 90° coupling of adjacent quadrupoles and explains the canting of the magnetic moments in the AFM phase as a result of competition between the 90° quadrupolar and the collinear AFM couplings, (2) it is compatible with the opposite displacements of the B and C atoms, and (3) it explains the induced magnetic structure for $\mathbf{H}\|[100]$. However, it does not explain (4) the absence of the (1 0 5/2) reflection in the AFQ phase measured with resonant x-ray diffraction in the $\sigma - \pi'$ geometry.[9] We suggest to study if translational quadrupolar domains related by the lost (001) translation would explain the x-ray results. Such antiphase domains should scatter coherently and have equal population.

The parallel arrangement of quadrupoles proposed by Matsumura *et al.*[9] seems to us less probable than the 90° arrangement. This model implies parallel quadrupolar couplings, which (1) do not frustrate collinear AFM couplings, so there should be no canting of the magnetic moments in the AFM phase according to this model. Such arrangement is compatible (2) with the same shifts of the B and C atoms, but (3) it has problems to explain differences of the $\mathbf{M_{1x}}$ and $\mathbf{M_{2x}}$ components of the induced magnetic structure in the AFQ phase. It explains, however, (4) the behavior of the (1 0 5/2) reflection in the x-ray experiment.[11]

The canted arrangement of quadrupoles proposed by Tanaka *et al.*[3] certainly exists in the AFM state below T_N. But we do not see why this scheme should be adopted unfounded for the AFQ state as well. This model implies that: (1) the AFM interactions are very significant already in the AFQ phase, forcing canting of the quadrupoles well above T_N, (2) it is very asymmetric relative to the shifts of the B and C atoms; and, finally (3) it is not clear why the $\mathbf{M_y}$ components of induced magnetic structure in the AFQ phase should compensate each other or (4) why the (1 0 5/2) reflection vanishes in the AFQ phase in the x-ray experiment.

IV. SUMMARY

We have investigated phase transitions in DyB_2C_2 by means of symmetry analysis and neutron diffraction of a $Dy^{11}B_2C_2$ single crystal. The τ_7 representation describes the AFQ phase. The transition at T_Q involves periodic displacements of the B and C atoms along the *z* axis and ordering of the Dy quadrupoles in the *xy* plane. The Dy ions do not shift from the initial positions. We suggest the 90° arrangement of neighboring quadrupoles in the *xy* plane and along the *z* axis in the AFQ phase and opposite shifts for the B and C atoms. The magnetic structure induced by $\mathbf{H}\|[100]$ in the AFQ phase comprises zero or compensating $\mathbf{M_y}$ and different $\mathbf{M_x}$ components.

The magnetic structure below T_N is described by the τ_9 representation. The neutron diffraction data are consistent with modified model A with the same value of magnetic moments for four Dy sublattices, but canting between them. At zero-field orientation, domains with equal population of this magnetic structure coexist. The magnetic exchange interaction of the neighboring Dy moments dominates the 90° quadrupolar interaction and leads to the canting of the quadrupoles within the *xy* plane, as proposed by Tanaka *et al.*[3] Magnetic field applied along $\mathbf{H}\|[100]$ destroys domains with net moment perpendicular to the field direction. Moreover, it suppresses the AFM couplings of the neighboring Dy magnetic moments in the preserved domain, and the Dy quadrupoles tend to restore the 90° arrangement.

Similar coexistence and competition of antiferroquadrupolar and antiferromagnetic interactions exist in other RB_2C_2 compounds [R=Ho (Ref. 36) and Tb (Ref. 37)]. We hope that our theoretical and experimental findings can be useful for the understanding of these phases as well.

ACKNOWLEDGMENTS

The work was performed on the TriCS instrument at SINQ, Paul Scherrer Institute, Villigen, Switzerland. We are grateful for helpful discussions with K. Katsumata, RIKEN Harima Institute, Japan. We acknowledge the expert technical assistance of Dr. M. Zolliker and Ch. Kägi, PSI. W.S. and F.B. are grateful to the State Committee for Scientific Research in Poland for partial financial support.

*Corresponding author. O. Zaharko, Laboratory for Neutron Scattering, ETHZ & PSI, CH-5232 Villigen, Switzerland; FAX: +41 56 310 2939. Electronic address: oksana.zaharko@psi.ch

[1] K. Ohoyama, K. Kaneko, K. Indoh, H. Yamauchi, A. Tobo, H. Onodera, and Y. Yamaguchi, J. Phys. Soc. Jpn. **70**, 3291 (2001).

[2] H. Yamauchi, H. Onodera, K. Ohoyama, T. Onimaru, M. Kosaka, M. Ohashi, and Y. Yamaguchi, J. Phys. Soc. Jpn. **68**, 2057 (1999).

[3] Y. Tanaka, T. Inami, T. Nakamura, H. Yamauchi, H. Onodera, K. Ohoyama, and Y. Yamaguchi, J. Phys.: Condens. Matter **11**, L505 (1999).

[4] K. Hirota, N. Oumi, T. Matsumura, H. Nakao, Y. Wakabayashi, Y. Murakami, and Y. Endoh, Phys. Rev. Lett. **84**, 2706 (2000).

[5] H. Adachi, H. Kawata, M. Mizumaki, T. Akao, M. Sato, N. Ikeda, Y. Tanaka, and H. Miwa, Phys. Rev. Lett. **89**, 206401 (2002).

[6] We refer to the crystallographic unit cell $a=b=5.346$ Å, $c=3.541$ Å throughout the paper to follow notations accepted in literature. However, we do not use two wave vectors to describe the AFQ order, $\mathbf{k_1}=[0,0,\frac{1}{2}]$ and $\mathbf{k_4}=[0,1,\frac{1}{2}]$, as is often done. This is because $\mathbf{k_4}$ produces the set of reflections which is a subset of the $\mathbf{k_1}$ set. The same holds for the wave vectors associated with the AFM order: $\mathbf{k_2}=[0,0,0]$ and $\mathbf{k_3}=[1,0,0]$. We use, therefore, only $\mathbf{k_1}$ and $\mathbf{k_2}$.

[7] T. Nakamura, U. Staub, Y. Narumi, K. Katsumata, and F. Juranyi, Europhys. Lett. **62**, 251 (2003).

[8] Here the coordinates of atoms are given in the $P4/mbm$ space group to follow Refs. 2 and 12.

[9] T. Matsumura, N. Oumi, K. Hirota, H. Nakao, Y. Murakami, Y. Wakabayashi, T. Arima, S. Ishihara, and Y. Endoh, Phys. Rev. B **65**, 094420 (2002).

[10] Y. Tanaka, T. Inami, S. W. Lovesey, K. S. Knight, F. Yakhou, D. Mannix, J. Kokubun, M. Kanazawa, K. Ishida, S. Nanao, T. Nakamura, H. Yamauchi, H. Onodera, K. Ohoyama, and Y. Yamaguchi, Phys. Rev. B **69**, 024417 (2004).

[11] S. W. Lovesey and K. S. Knight, Phys. Rev. B **64**, 094401 (2001).

[12] J. van Duijn, J. P. Attfield, and K. Suzuki, Phys. Rev. B **62**, 6410 (2000).

[13] N. Fukushima and Y. Kuramoto, J. Phys. Soc. Jpn. **67**, 2460 (1998).

[14] H. Yamauchi, K. Ohoyama, M. Sato, S. Katano, H. Onodera, and Y. Yamaguchi, J. Phys. Soc. Jpn. Suppl. **71**, 94 (2002).

[15] H. Yamauchi, K. Ohoyama, S. Katano, M. Matsuda, K. Indoh, H. Onodera, and Y. Yamaguchi, J. Phys.: Condens. Matter **15**, S2137 (2003).

[16] S. Sako, H. Onodera, H. Yamauchi, K. Indoh, A. Tobo, K. Ohoyama, and Y. Yamaguchi, J. Phys. Soc. Jpn. **69**, 1872 (2000).

[17] E. F. Bertaut, J. Appl. Phys. **33**, 1138 (1962).

[18] E. F. Bertaut, Acta Crystallogr., Sect. A: Cryst. Phys., Diffr., Theor. Gen. Crystallogr. **24**, A217 (1968).

[19] E. F. Bertaut, J. Phys. Colloq. **1**, 462 (1971).

[20] E. F. Bertaut, J. Magn. Magn. Mater. **24**, 267 (1981).

[21] Yu. A. Izyumov, V. E. Naish, and R. P. Ozerov, *Neutron Diffraction of Magnetic Materials* (Consultants Bureau, New York, 1991).

[22] W. Sikora, L. Pytlik, and F. Bialas, *Neutron Scattering and Complementary Methods in Investigations of Condensed Phase*, edited by J. Chrusciel (University of Podlasie, Siedlce, 2003), p. 50; http://novell.ftj.agh.edu.pl/~sikora/modyopis.htm

[23] It is worth noting that some arguments of Ref. 11 are wrong. (i) The assumption about displacements of the B and C atoms by $z=0.05$ corresponds to 0.177Å shifts. This is unreasonably large. Reasonable values would be at least one order of magnitude less and they cannot be extracted from powder neutron diffraction patterns of Ref. 2 due to too small sin θ/λ range and medium

resolution. (ii) In the $P4_2/mnm$ space group the actual 4(*c*) site, as well as the 8(*h*) site allowing *z* shifts for the Dy ion, contribute only to *hkl* with $h+k,l=2n$, so they do not contribute to $(1\ 0\ l/2)$ reflections.

[24] Y. Tanaka, Y. Tabata, K. Katsumata, K. Tamasaku, T. Ishikawa, N. Kawamura, M. Suzuki, H. A. Katori, S. W. Lovesey, H. Yamauchi, H. Onodera, and Y. Yamaguchi, J. Phys.: Condens. Matter **15**, L185 (2003).

[25] For completeness we performed also the symmetry analysis for the space group $P4/mbm$. The results did not lead to models of magnetic structures proposed from neutron experiment (Refs. 2 and 12). The Dy1 at (0 0 0) and Dy2 $(\frac{1}{2}\ \frac{1}{2}\ 0)$ ions belong to the same crystallographic site 2(*a*). The magnetic wave vector $\mathbf{k_1}=[0,0,\frac{1}{2}]$ does not split this position and magnetic moments of Dy1 and Dy2 ions must be symmetry related. The same holds for Dy3 $(0\ 0\ \frac{1}{2})$ and Dy4 $(\frac{1}{2}\ \frac{1}{2}\ \frac{1}{2})$ ions from the 2(*b*) site. However, neither model A nor B obeys this constraint.

[26] P. J. Brown, Physica B **192**, 14 (1993).

[27] V. Petricek, and M. Dusek, *JANA2000 The Cystallographic Computing System* (Institute of Physics, Praha, Czech Republic, 2000).

[28] J. Rodriguez-Carvajal, Physica B **192**, 55 (1993).

[29] The collected data set at 30 K was too small to verify the space group and to refine the positions of atoms.

[30] The refined magnetic moment value is $5.7(4)\mu_B$/Dy, which is lower than the values obtained in previous studies: $7.1(1)\mu_B/\mathrm{Dy}^2$ and $8.3(6)\mu_B$/Dy (Ref. 12). We attribute this discrepancy to higher temperature of our experiment (12 K) compared to 2.2 K (Ref. 2) and 4 K (Ref. 12).

[31] K. Kaneko, S. Katano, M. Matsuda, K. Ohoyama, H. Onodera, and Y. Yamaguchi, Appl. Phys. A: Mater. Sci. Process. **74**, 1749 (2002).

[32] K. Indoh, H. Onodera, H. Yamauchi, H. Kobayashi, and Y. Yamaguchi, J. Phys. Soc. Jpn. **69**, 1978 (2000).

[33] K. W. H. Stevens, Proc. Phys. Soc., London, Sect. A **65**, 209 (1952).

[34] R. Shiina, H. Shiba, and P. Thalmeier, J. Phys. Soc. Jpn. **66**, 1741 (1997).

[35] The increase of magnetic moment along the field direction in the AFQ state has been deduced also in Ref. 15 from the ratio of intensities $I_{10\ 1/2}/I_{101}$ for $\mathbf{H}\|[010]$. However, the authors considered only the canted arrangement of quadrupoles to interpret this observation. The same arrangement has been postulated in the publication which appeared recently: K. Indoh, A. Tobo, H. Yamauchi, K. Ohoyama, and H. Onodera, J. Phys. Soc. Jpn. **73**, 669 (2004).

[36] K. Ohoyama, H. Yamauchi, A. Tobo, H. Onodera, H. Kadowaki, and Y. Yamaguchi, J. Phys. Soc. Jpn. **69**, 3401 (2000).

[37] K. Kaneko, H. Onodera, H. Yamauchi, T. Sakon, M. Motokawa, and Y. Yamaguchi, Phys. Rev. B **68**, 012401 (2003).